ASTRONOMY & ASTROPHYSICS
SUPPLEMENT SERIES

Astron. Astrophys. Suppl. Ser. **126,** 161-167 (1997)

Spectral detector for interference time blanking using quantized correlator

R. Weber [1], **C. Faye** [2], **F. Biraud** [3], **and J. Dansou** [4]

1 LESI-ESPEO, Université d'Orléans, 45000 Orléans, France
2 ETIS-ENSEA, 95000 Cergy-Pontoise, France
3 Unité Scientifique de Nançay, Observatoire de Paris, 1 Place Jules Janssen, F-92195 Meudon Principal Cedex, France
4 GTR-IUT de Blois, 41 000 Blois, France

Received December 10, 1996; accepted February 21, 1997

Abstract. Given the large flow of data to be processed, quantized correlators are widely used in radio astronomy. Unfortunately, the occurrence of non-Gaussian interference combined with a coarse quantization can strongly alter the shape of the estimated spectra. The final spectral estimation can be preserved by blanking the correlator in real-time. A new interference detection criterion is proposed within this framework. It uses the real-time capabilities of correlators and compares contaminated and non-contaminated correlation functions. No a priori information on the interfering signals is required. Simulations, using synthetic and actual data, are presented. This new technique of real time detection can significantly improve the quality of spectral line observations.

Key words: instrumentation: miscellaneous — methods: data analysis — techniques: spectroscopic

1. Introduction

The negative impact of radio frequency interference (RFI) on the quality of spectral lines observations (see examples in Fig. 1) is a matter of increasing concern for the radio astronomy community (McNally 1994; Daigne 1994). Among the various observation techniques, non-interferometric receivers are the most vulnerable, and methods to preserve observation capabilities are urgently required (Gérard 1993; Thompson et al. 1991).

However, very few practical and efficient solutions have been proposed so far (cf. NRAO 1982; Lacasse 1993). The problem is compounded when highly quantized correlators (1 to 3 bits) are used to estimate spectra. Preliminary work, performed at the Nançay Observatory (to be published), has shown that the occurrence of non-Gaussian interferences may considerably alter the shape of estimated spectra:

Let us define the INR (Interference to Noise Ratio) as the interference power divided by the total system noise power in the receiver bandwidth, and let us consider the case of a 1-bit correlator and a sinusoidal RFI. The interference level detrimental to radioastronomy adopted by the ITU (see, e.g., Recommendation ITU-R RA 769) gives a response equal to 0.1 of the rms noise fluctuations after 2000 seconds of integration. For a spectral line observation in L-band, a typical bandwidth is 20 kHz. The INR is then -48 dB.

We determined that for an INR below -10 dB, the effects of interference are not exacerbated by the non-linearity of coarse quantization. In particular, the harmonics generated can be neglected, as their level is typically 50 dB below the noise power. This allows suppression or reduction of the interfering signal by off-line processing (an example is given in Fig. 2). For INR exceeding -10 dB, however, it becomes necessary to detect the presence of RFI before conducting the spectral estimation. The acquisition process is then momentarily suspended to prevent contamination of previously stored data. Consequently the final spectrum is preserved, free of distorsions, and, too large RFI are suppressed.

In this paper, the concept of a spectral detector is introduced. It is based on the comparison between the spectral and statistical profiles of the measured —and possibly disturbed— noise $s(t)$, and that of an undisturbed Gaussian noise delivered by a noise generator placed at the input of the receiver. One of the main advantages of the proposed detector is its tolerance of short and medium term non stationarity. This usually affects the measured noise due to changing observation conditions, namely antenna or earth rotation. It uses the concept of a generalized chi-square test (Moulines et al. 1993) applied to second

Send offprint requests to: R. Weber
e-mail: weber@lesi.univ-orleans.fr

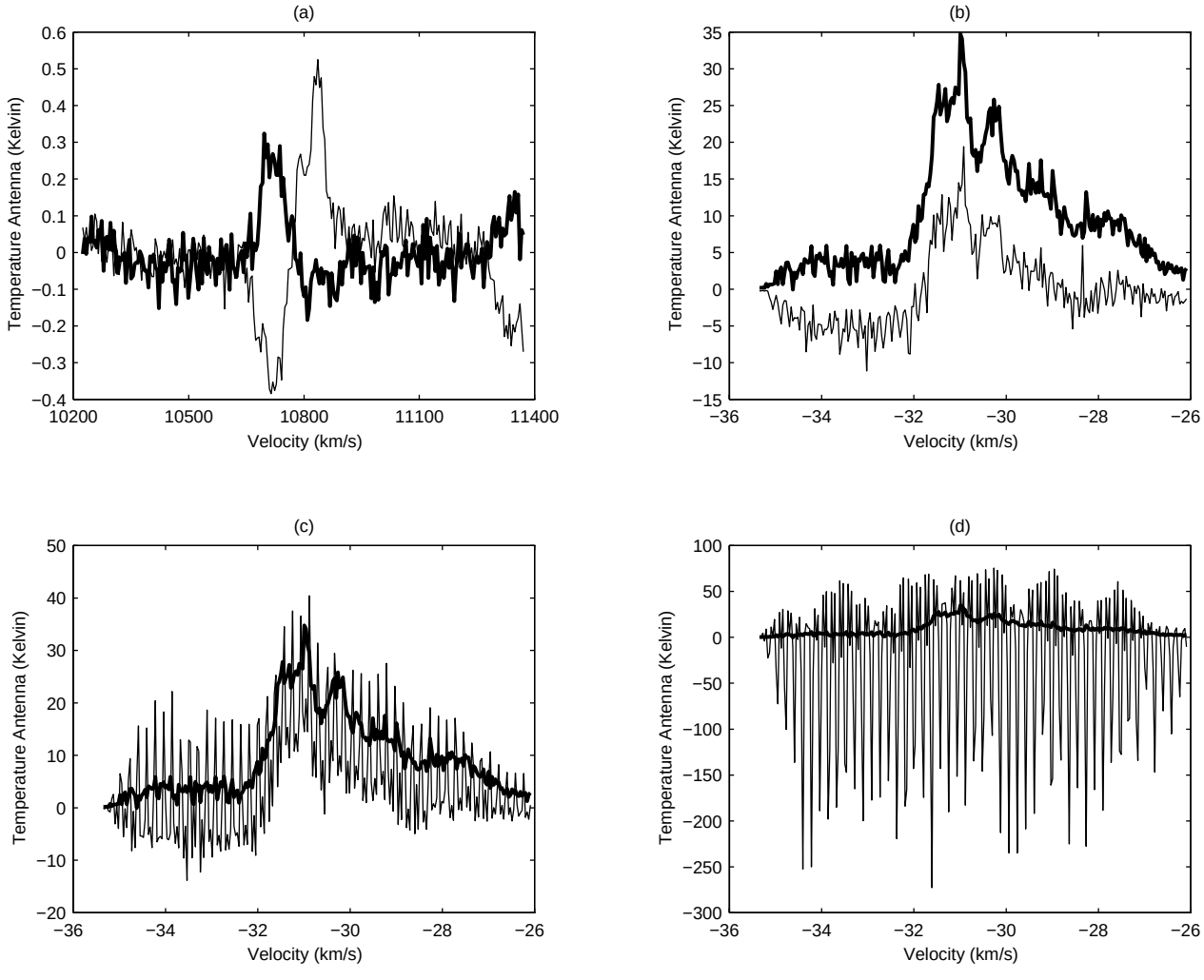

Fig. 1. Spectra of the OH radical measured with the Nançay Decimetric Radio Telescope (NRT) and polluted by spread spectrum RFI. The thick line represents the expected profile and the thin line represents the contaminated one: **a-c)** redshifted 1667 MHz profile of the galaxy Markarian 273, **d)** circumstellar envelope of the late-type star OH 104.9

order moments of $s(t)$. The proposed implementation takes advantage of the real time capabilities of existing correlators.

2. Generalized chi-square test (χ^2) theory

This test is based on the evaluation of the quadratic error between *sample mean* and *ensemble averaged* values of Q non-linear functions of the observations:

Let $s_{\rm n}$ be the discrete version of the measured noise $s(t)$. From a set of non-linear L_k-variate functions F_k and from appropriate choice of L_k time-lags $\tau_{i,k}$, a set of Q *sample mean* generalized moments, w_k, are computed on N successive samples. The general form of such a *sample mean* value can be written as:

$$w_k = \frac{1}{N}\sum_{j=0}^{N-1} F_k(s_{j-\tau_{1,k}}, s_{j-\tau_{2,k}}, \cdots, s_{j-\tau_{L_k,k}}) \qquad (1)$$

where $k = 1, \ldots, Q$.

Let $\mathbf{X}$ denote the Q-dimensional vector formed by the juxtaposition of the *sample mean* w_k:

$$\mathbf{X} = [w_1, w_2, \cdots, w_Q]^t \qquad (2)$$

where $[\ ]^t$ symbolizes the transpose operator.

When the noise $s(t)$ is free of RFI (termed the $\mathcal{H}_0$ hypothesis throughout this paper), this vector $\mathbf{X}$ converges to a multivariate Gaussian variable with *ensemble average* mean vector $\mathbf{X}_0$ and *ensemble average* covariance matrix $\mathbf{R_0}$ (Moulines et al. 1993). $\mathbf{X}_0$ and $\mathbf{R_0}$ depend on the statistical properties of the noise under the $\mathcal{H}_0$ hypothesis. In the present case, under the $\mathcal{H}_0$ hypothesis, the noise is assumed to be Gaussian. Thus, only the second order statistical properties are involved.

The test function $\mathcal{C}(s)$ consists in computing the quadratic error between the measured $\mathbf{X}$ and the expected $\mathbf{X}_0$. To normalize and take the statistical links between the

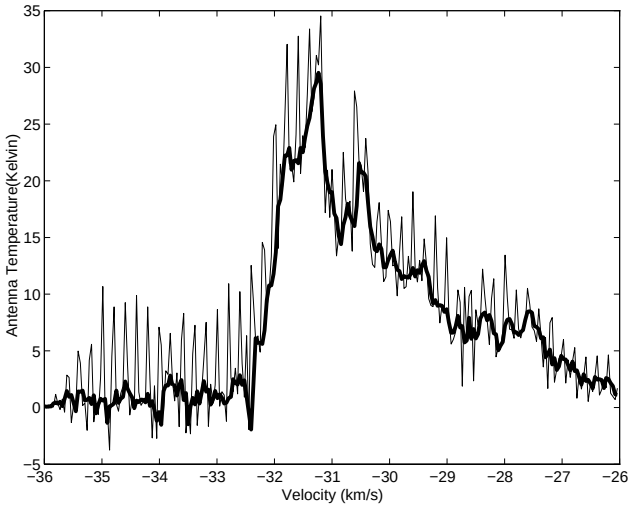

Fig. 2. An example of RFI suppression by off-line processing. The thin line represents the contaminated profile and the thick line represents the clean one. In this specific example, the RFI spectral charateristics are sufficiently narrow to be excised by using a median filter and an interpolation method (NRAO 1982) (Kasparis & Lane 1993)

w_k into account, this quadratic error is weighted by the inverse of the covariance matrix $\mathbf{R_0}$. Namely,

$$\mathcal{C}(s) = (\mathbf{X} - \mathbf{X_0})^{\mathbf{t}} \mathbf{R_0^{-1}} (\mathbf{X} - \mathbf{X_0}). \quad (3)$$

Under the $\mathcal{H}_0$ hypothesis, the test function $\mathcal{C}(s)$ is distributed asymptotically as a central chi-square variable whose degree of freedom is related to vector size Q. When no parameter of the $s(t)$ statistics needs to be estimated, the degree of freedom is exactly Q (Moulines et al. 1993). Knowing the test distribution under the $\mathcal{H}_0$ hypothesis, it is easy to establish a detection level λ as a function of the desired false alarm probability.

3. Application of χ^2 to RFI detection

The idea is to use the real time capabilities of the correlators to compute the vector $\mathbf{X}$.

Denote $g(x_1, x_2)$ as the quantized product between level x_1 and level x_2; and l_i the quantization levels. When $l_i < x_1 \leq l_{i+1}$ and $l_j < x_2 \leq l_{j+1}$, the value of the quantized product $g(x_1, x_2)$ is given by $m_{i,j}$. Table 1 gives an example of a quantization scheme. By the means of $g(x_1, x_2)$, a set of Q bivariate ($L_k = 2$) non-linear functions F_k can be obtained, namely:

$$F_k(s_j, s_{j-\tau_k}) = g(s_j, s_{j-\tau_k}) \ , \ k = 1, \ldots, Q. \quad (4)$$

By taking the mean of these functions, the generalized moments, w_k, given by Eq. (1) and the vector $\mathbf{X}$ given by Eq. (2) are generated. In fact, the proposed vector $\mathbf{X}$ corresponds to Q time-lags of the quantized correlator and it is instantaneously obtained through the correlator buffers after N clock cycles. Thus, only the matrix operations of Eq. (3) need to be externally calculated in real time.

These matrix operations use the knowledge of the reference vector $\mathbf{X}_0$ and the covariance matrix $\mathbf{R_0}$. In practice, the latter are estimated from the observations. This point is addressed in the following section.

4. Evaluation of the reference vector $\mathbf{X_0}$ and the covariance matrix $\mathbf{R_0}$

4.1. Hypothesis

Under the $\mathcal{H}_0$ hypothesis, the noise $s(t)$ is assumed to be Gaussian. $\mathbf{X}_0$ and $\mathbf{R_0}$ are characterized by the total power σ^2 and the normalized autocorrelation function $\overline{\rho}(\tau) = \rho(\tau)/\sigma^2$ of the noise $s(t)$.

From a practical point of view, $\overline{\rho}(\tau)$ depends mainly on the receiver (e.g. the successive filter shapes). Other contributions to the final spectral shape can be considered either locally white (e.g. the ground noise) or negligible (e.g. the cosmic source). Moreover, $\overline{\rho}(\tau)$ being stationary over large durations (>1 hour), it will be estimated once at the beginning of the observation by using a noise generator as a virtual non-contaminated source (see Sect. 5).

With regard to σ^2, due to antenna or earth rotation, stationarity can not be guaranteed beyond a few minutes. It is therefore necessary to take into account the current σ^2 value when computing $\mathcal{C}(s)$.

4.2. Method

Because of the quantization process, the dependence of $\mathbf{X}_0$ and $\mathbf{R_0}$ on σ^2 is not simple. Moreover, the number of operations required to estimate the test function $\mathcal{C}(s)$ is proportional to Q^2. This can restrain the real time capabilities for large Q. To circumvent these drawbacks, it is necessary, firstly, to take into account the dependence on σ^2 in *an easy way* and, secondly, to reduce the impact of the $Q \times Q$ matrix $\mathbf{R}_0^{-1}$ on the computational time.

Knowing the normalized autocorrelation function $\overline{\rho}(\tau)$ for each involved time lag, the reference vector $\mathbf{X}_0$ depends only on σ^2:

$$\mathbf{X}_0(\sigma^2) = \left[\sum_i \sum_j m_{i,j} P_{i,j}(\overline{\rho}(\tau_1), \sigma^2), \ldots \right.$$
$$\left. \ldots, \sum_i \sum_j m_{i,j} P_{i,j}(\overline{\rho}(\tau_Q), \sigma^2) \right]^t \quad (5)$$

where $P_{i,j}(\overline{\rho}, \sigma^2)$ is the joint probability that two Gaussian variables with zero mean, equal variance σ^2, and with normalized correlation coefficient $\overline{\rho}$ belong to the $[l_i, l_{i+1}] \times [l_j, l_{j+1}]$ area.

So, the $\mathbf{X}_0$ variation with σ^2 will be given by Q (one for each component of the vector), second order polynomial

approximations of Eq. (5). These approximations must be valid within the expected fluctuation domain of σ^2 under the $\mathcal{H}_0$ hypothesis.

A general formula for $\mathbf{R}_0$ is complicated by the correlation between the samples s_n. One solution is to keep the sample uncorrelated by forcing the Nyquist property (Nyquist 1928) on the noise under the $\mathcal{H}_0$ hypothesis. Generally, this can be achieved by slightly modifying the receiver spectral shape, so that the periodic zeros in the correlation function occur at a known periodicity. Independence between samples can be guaranteed by sampling the noise with this known rate. This method leads to an exact and computable $\mathbf{R}_0$ formula but requires some modifications of the receiver.

An alternative solution would be to neglect the dependence between samples and to simply consider the noise under the $\mathcal{H}_0$ hypothesis as a white noise despite its band limitation. This simplification induces to a change in the weighting factors of the errors between the $\mathbf{X}$ and $\mathbf{X}_0$ components and makes the criterion less than optimal.

Under either of these previous hypotheses, the matrix $\mathbf{R}_0$ becomes diagonal:

$$\mathbf{R_0}(\sigma^2) = \frac{1}{N} \sum_i \sum_j m_{i,j}^2 P_{i,j}(0, \sigma^2)\mathbf{I} \tag{6}$$

where $\mathbf{I}$ is the unit matrix.

Therefore, no matrix inversion is needed and the number of operations necessary to compute the test function $\mathcal{C}(s)$ becomes proportional to Q. Furthermore, its variation with σ^2 can be computed as a second order polynomial approximation. $\mathcal{C}(s)$ becomes a classical quadratic mean error test.

Table 1. Technical features of the NRT quantized correlator. Because of symmetry, only 1/2 of the quantization levels and 1/4 of the product table are given

$g(x_1, x_2)$	
Quantization levels l_i $(\sigma^2 = 1)$	(0 0.436 1.017 1.67)
Product table $m_{i,j}$	1 3 6 8 1 2 4 6 0 1 2 3 0 0 1 1

5. Implementation

5.1. Presentation

In this section, a method to implement the previous detection criterion is proposed (see Fig. 3). The criterion uses the first Q time lag ($\tau_k = k$) of the quantized correlation function $R(\tau)$. To initialize the detector, knowledge of the receiver spectral shape is necessary. Thus, at the beginning of the observation, the receiver is directly connected to a noise generator so that the $\mathcal{H}_0$ hypothesis is forced. The quantized autocorrelation $R(\tau)$ is estimated and the true normalized autorrelation, $\overline{\rho}(\tau)$, is deduced from $R(\tau)$ by applying the correlation correction function (Hagen & Farley 1973). Then, the coefficients of the second order polynomial approximations, used to evaluate the $\mathbf{X}_0$ and $\mathbf{R_0}$ dependance on σ^2, are computed and stored.

The receiving system is then connected to the antenna, and observation starts. At each clock cycle, the Q values of the quantized product for the Q first time lags are computed by the correlator and stored into Q shift registers of size N. For each time-lag, these shift registers represent a moving window on the N last quantized products used to compute the final vector $\mathbf{X}$.

The component w_0, which is issued from the null time-lag and is an estimate of the input power σ^2 (see note 1), is used to update $\mathbf{X}_0$ and $\mathbf{R_0}$. Then, the test function $\mathcal{C}(s)$ is computed and its value is compared with the predefined detection level λ. If the test function value is less than λ, no RFI is detected, and the "first in" quantized products are sent to the final integration. If the criterion value is greater, an RFI is detected and the final sum is suspended until the test function value comes down below the detection level again.

The size of the implementation depends on the size Q of the vector $\mathbf{X}$. In the next section, the influence of Q on the detector is demonstrated.

5.2. Choice of the size Q of the vector X

For a given RFI, the choice of the size Q strongly determines the detector performance. From a spectral point of view, the detector carries out a comparison between an estimated spectrum and a reference spectrum with a spectral resolution inversely proportional to Q. By using values of Q which are too small, the risk is the smoothing of relevant spectral features of the RFI and therefore reduction in the quadratic error between $\mathbf{X}$ and the reference $\mathbf{X}_0$. In contrast, large values of Q may reduce the detector performance because of a large induced variance[2]. In fact, the optimal value of Q must be chosen as a function of RFI and the observational context.

Nevertheless, for multiple RFI detection or blind detection (no a priori information on RFI), the proposed detector can be modified to perform multiresolution criteria: the detector is sized for the largest value of Q (highest resolution) and criteria with intermediate resolution are obtained recursively.

[1] w_0 and σ^2 are linked together by $w_0 = \sum_i m_{i,i} P_i(\sigma^2)$ where $P_i(\sigma^2)$ is the probability that a Gaussian variable with zero mean and variance σ^2, belongs to the $[l_i, l_{i+1}]$ interval.

[2] The variance of chi-square law is proportional to the degree of freedom, which is approximatively Q in the present case.

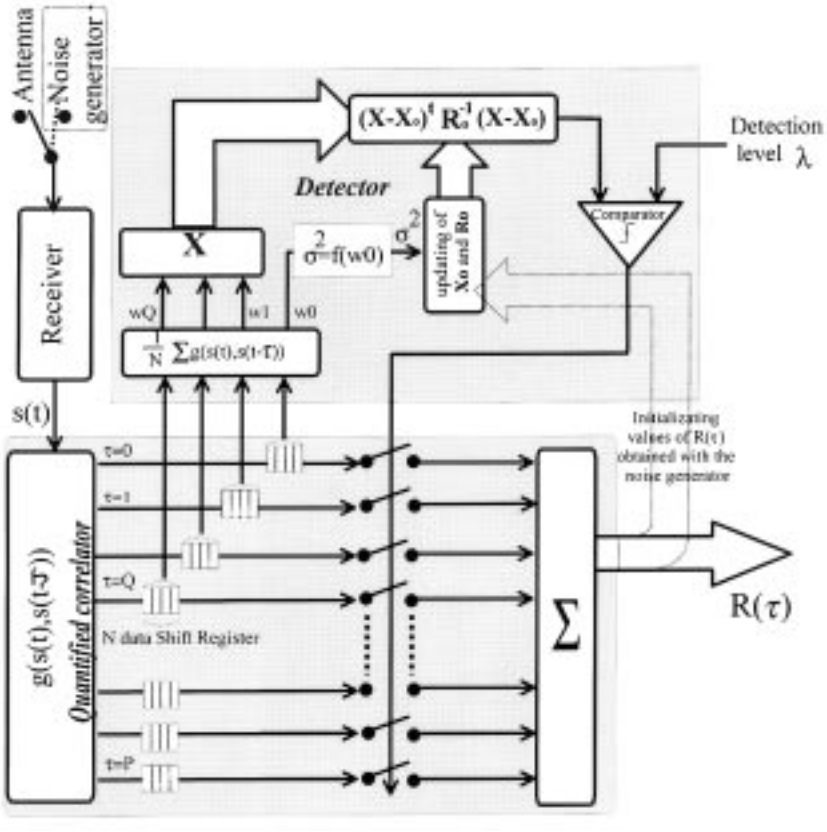

Fig. 3. Implementation of the detector (dotted lines represent the initialisation phase). The test function uses the Q first channels of a P channels correlator

6. Performances

6.1. Hypothesis

The purpose of this section is to evaluate the performance of the proposed detector. The number of samples, N, and the size Q of the vector $\mathbf{X}$ have been fixed respectively at 10000 and 30. Under the $\mathcal{H}_0$ hypothesis, the noise is Gaussian and its spectral shape is given in Fig. 4. All the numerical processing, including the quantized autocorrelation, has been simulated numerically. The quantization parameters are those given in Table 1. The tests were made, first on synthetic data and, then, on actual data acquired by the Nançay Decimetric Radio Telescope (NRT).

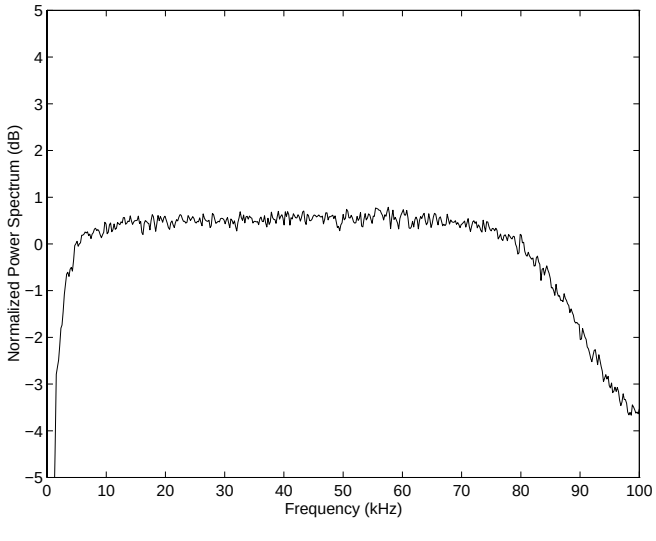

Fig. 4. Spectrum of the noise under the $\mathcal{H}_0$ hypothesis. This typical shape has been measured from the NRT receiver

6.2. Tests with synthetic data

Three typical RFI were chosen for the tests : a sine wave (SW), and two filtered spread spectrum signals with two kinds of band limitation (see Fig. 5). The performance analysis is based on hypothesis testing. Two cases are possible, whether the RFI is present ($\mathcal{H}_1$ hypothesis) or not ($\mathcal{H}_0$ hypothesis). In order to obtain the needed probabilities of detection P_{D} and probabilities of false alarm P_{FA}, it is necessary to generate many sample paths of the involved data. For the results presented here, 800 sample paths for each hypothesis were generated. Figure 6 shows

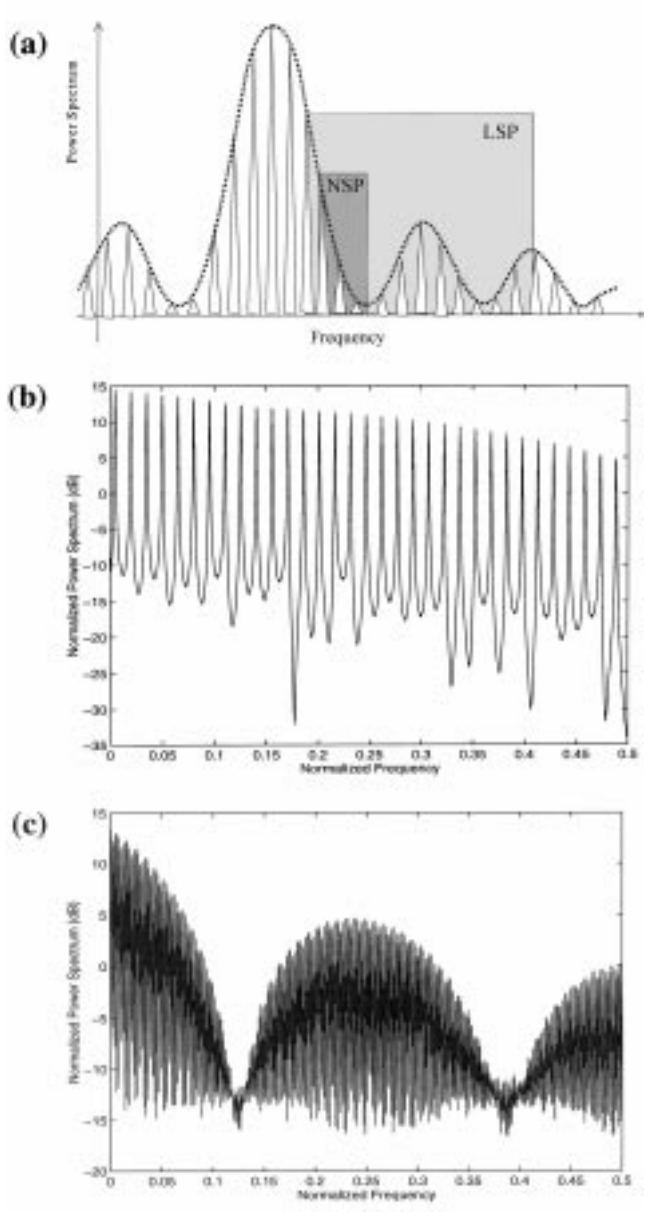

Fig. 5. Spectra of the spread spectrum RFI. They are extracted from spectra similar to those generated by Global Positioning System (GPS) or Global Navigation Satellite System (GLONASS): **a)** spectrum of a spread spectrum signal, **b)** spectrum of the tested narrow band filtered spread spectrum RFI (NSP), **c)** spectrum of the tested large band filtered spread spectrum RFI (LSP)

the plots of P_{FA} against P_{D} (ROC curves[3]) for the three types of RFI retained. The aim was to find the smallest INR (< -10 dB) which yields at least a P_{D} superior to 95% with a P_{FA} inferior to 5%.

This objective is outperformed in the sine wave case, since an INR of -17 dB is reached. For the spread spectrum cases, the performance decreases. The large band

[3] Receiver operating characteristics.

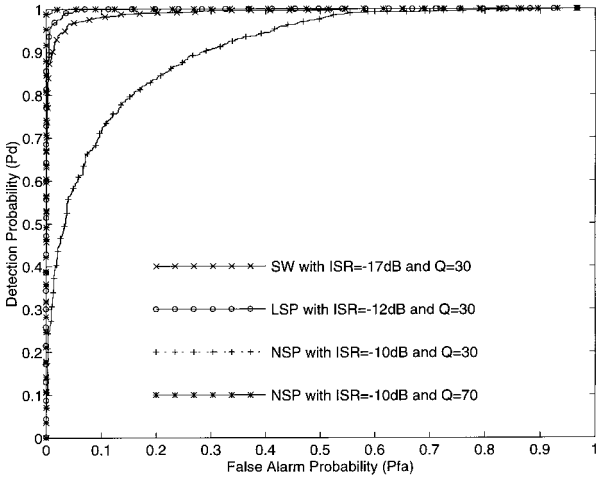

Fig. 6. P_{FA} against P_{D} for the three types of RFI retained: a sine wave (SW), a narrow band filtered spread spectrum RFI (NSP), a large band filtered spread spectrum RFI (LSP). $N = 10000$ samples are used for each one of the 800 trials. Q is the size of the test vector $\mathbf{X}$

spread spectrum (LSP) case is still detected well with a level of -12 dB but the narrow band spread spectrum (NSP) case does not reach the limit of -10 dB. These performance differences are related to the spectral appearance of the RFI when they are observed through a resolution of $1/Q$ (see Sect. 5.2). With $Q = 30$, the NSP case appears spectrally as a white noise, thereby diminishing the detection capabilities. By increasing the resolution, the detection is improved (see Fig. 6 with $Q = 70$).

6.3. Tests with real data

To validate the results obtained with simulated data and verify the likelihood of the $\mathcal{H}_0$ hypothesis, the noise delivered by the receiver was sampled at a rate of 200 kHz during 10 s. A dedicated RFI generator (see images available on the electronic version of the paper) was used to emit the retained three types of RFI.

Firstly, the measured ROC curves were similar to those obtained with synthetic data. This comparison has validated the hypothesis made on the noise under the $\mathcal{H}_0$ hypothesis. Secondly, a practical test was made. The RFI generator was turned on and off manually at random times and for random durations. The power of RFI was adjusted to deliver an INR of -10 dB. The same algorithm (defined in Sect. 5) was applied to the stored data, the detection threshold being chosen to guarantee a P_{FA} of 5%. The detection window was fixed at 50 ms ($N = 10000$ samples). When an RFI was detected, the corresponding data were discarded from the final integration. The resulting spectra are shown in Fig. 7. In both cases, the final spectrum shows significant improvement.

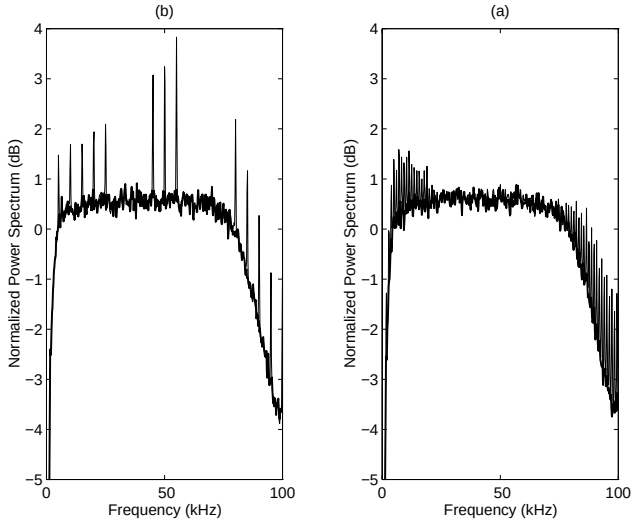

Fig. 7. Experimental spectra resulting from the NRT receiver. They are measured over 10 s on a 100 kHz band without (thin lines) and with time-blanking (thick lines) processing. Detection time = 50 ms (equivalent to $N = 10000$ samples), $P_{\mathrm{FA}} = 5\%$, $Q = 30$, INR $= -10$ dB: **a)** 12 sine waves RFI (SW), **b)** 2 large band spread spectrum RFI (LSP)

6.4. Asymptotic performances

In this section, the asymptotic performance is evaluated as a function of INR and N. As shown in Sect. 5.2, the dependance on Q is strongly linked with the RFI spectral appearance and is not included in this analysis. Equation (6) shows that $\mathbf{R}_0^{-1}$ is proportional to N. When INR is low (< -10 dB) the quantized correlator can be considered as linear. Consequently, the term $\mathbf{X} - \mathbf{X}_0$ of Eq. (3) is proportional to INR. Thus, the criterion $\mathcal{C}(s)$ is proportional to $N(\mathrm{INR})^2$. For example, if the detection time is increased by a factor 100, a sine wave with an INR of -27 dB can be detected with a P_{D} of 95% and a P_{FA} of 5%.

6.5. Test with higher order moments

In the application presented here, only the second order statistics of $s(t)$ are tested. Nevertheless, it is also possible to exploit higher order statistics of $s(t)$ through the correlator. In this case, some channels of the correlator must be devoted to the computation of these higher order tests. For example, tests on the 3$^{\mathrm{rd}}$ or 4$^{\mathrm{th}}$ order statistics can be performed by feeding the correlator with $s(t)$ and its square version $s^2(t)$. Then, the non-linear functions are:

$$\begin{aligned} F_k^3(s_i, \alpha s_{i-k}^2 + \beta) &= g(s_i, \alpha s_{i-k}^2 + \beta) \\ F_k^4(\alpha s_i^2 + \beta, \alpha s_{i-k}^2 + \beta) &= g(\alpha s_i^2 + \beta, \alpha s_{i-k}^2 + \beta) \end{aligned} \quad (7)$$

where α and β are parameters used to center and to normalize $s^2(t)$ in relation to the quantization levels. Unfortunately, simulations for low INR (< -10 dB) have shown that performance is not improved compared with the second order case given by Eq. (4). In fact, such modifications of $\mathbf{X}$ increase its variance without increasing the difference between itself and the reference vector $\mathbf{X_0}$.

7. Conclusion

In this article, an RFI detector is proposed which is based on a spectral profile comparison. Real time detection is provided by taking advantage of the existing computational capability of correlators. For example, monochromatic RFI having an INR $= -17$ dB are detected. This requires only $Q = 30$ time-lags of the correlation function estimated over $N = 10000$ samples.

This study was made in the framework of the coarse quantized correlators, which are in current use in the radio astronomy community. However, the proposed application can be extended to any type of correlators. To limit the impact of the RFI spectral appearance, a multi-resolution strategy is proposed. A later version of this detector could adopt a multi-scale strategy with the aim of minimizing the receiver blanking according to RFI duration.

Acknowledgements. The authors gratefully acknowledge C. Fabrice and L. Denis for their assistance in performing the tests with experimental data. The Nançay Radio Observatory is the Unité Scientifique Nançay of the Observatoire de Paris, associated as Unité de Service et de Recherche (USR) No. B704 to the French Centre National de Recherche Scientifique (CNRS). The Nançay Observatory also gratefully acknowledges the financial support of the Conseil Régional of the Région Centre in France.

References

Daigne G., 1994, L'Astronomie 107, 194
Gérard E., 1993, La Vie des Sciences Comptes rendus série générale 10, 175
Hagen J.B, Farley D.T., 1973, Radio Sci. 8, 775
Kasparis T., Lane J., 1993, Electr. Let. 29, 22, 1926
Lacasse R., 1993, Proc. Workshop on New Generation Digital Correlators, N.R.A.O.
McNally D., 1994, The vanishing universe. Cambridge Univ. Press, p. 71
Moulines E., Dalle Molle J.W., Choukri K., Charbit M., 1993, IEEE Proc. H.O.S., p. 336
NRAO, 1982, Proc. Workshop Interference Identification and Excision, N.R.A.O.
Nyquist H., 1928, Trans. AIEE 47, 617
Thompson A.R., Gergely T.E, Vanden Bout P.A., 1991, Phys. Today, 41